Acoustic Surveillance Using an Unmanned Blended Wing Glider

Scott Mahar[1], Gerald D'Spain[2]

[1]3550 General Atomics Court, San Diego, CA 92121
[2]Retired Scripps Institution of Oceanography, La Jolla, CA

Scott Mahar, 3550 General Atomics Court, San Diego, CA 92121, Scott.Mahar@GA.com

Abstract: *Unmanned underwater vehicles (UUV) are efficient task multipliers, able to perform underwater surveillance and monitoring, while freeing manned platforms to perform more complex work. Through optimizing the UUV as a blended wing glider with forward propulsion provided by an intermittently operated buoyancy engine, the acoustic and electromagnetic signatures are drastically reduced, while the endurance and range of the vehicle is significantly increased. Additionally, higher energy density systems such as fuel cell systems can further advance the surveillance capabilities of a UUV.*

General Atomics Electromagnetic Systems (GA-EMS) is developing and testing a novel fuel cell powered UUV: a large, blended wing glider, optimized for stealth with extended transit and zero surface expression. GA-EMS has hybridized an existing 20-foot blended wing glider with a fuel cell system and is presently testing this system at-sea. The glider's wingspan enables spatially separated towed arrays, as well as fixed horizontal and vertical arrays on the leading edges and in the tail. Data from at-sea testing will be presented, showing the ability of the blended-wing glider to resolve signal location and elevation angle of a controlled underwater source.

GA-EMS is also optimizing and fabricating a next generation 20-foot blended wing glider, due to be completed in 2025. At this wingspan, the glider can be easily handled, launched, and recovered for a modest cost, while still performing relevant surveillance missions; a

much larger glider is envisioned for a final product. This next generation glider will include a sizable payload volume with the ability to transport and deploy novel surveillance systems. Aspects of the design of this next-generation glider will be presented.

Keywords: *UUV, Glider, surveillance, hydrophone, LiFT^{TM}, fuel cell, hydrodynamic, range, persistence*

EXECUTIVE SUMMARY

Blended-wing gliders are the ideal unmanned underwater vehicles (UUV) for persistent acoustic surveillance due to the lack of a continuously running propulsor and low hydrodynamic noise. Optimization of the glider's shape and integration of novel energy-dense systems enhance the persistence of the glider. General Atomics Electromagnetic Systems (GA-EMS) has been developing power and energy systems for UUVs and working with Scripps Institution of Oceanography (SIO) Marine Physical Laboratory (MPL) at the University of California San Diego (UCSD) to optimize the design and acoustic sensing capabilities blended wing gliders. The team continues to modify and test the existing 20-foot ZRay glider, as well as design and fabricate a next generation glider (GRay). The team is working to scale up the vehicle to a large wingspan which will enable large acoustic sensor layouts in multiple dimensions, leading to novel acoustic sensing capabilities.

INTRODUCTION

Buoyancy-driven gliders propel themselves by changing the buoyancy of the vehicle, either by changing the mass (amount of water in ballast tanks), or by changing the volume of the vehicle using bladders. This change in buoyancy changes the vehicle's potential energy in the earth's gravitational field, which is converted to kinetic energy as the glider descends (or ascends) through the water column. At the top of the dive cycle, the vehicle pumps in water (or reduces its volume) to make it denser than the surrounding water and begins its descent. At the bottom of the dive cycle, the vehicle pumps water out of the ballast tanks (or increases its volume) to be less dense than the surrounding water and ascends.

In 2004, SIO partnered with Applied Physics Lab at the University of Washington under sponsorship of the Office of Naval Research to design, fabricate, and test blended wing gliders [1]. Throughout the development program, the XRay glider was tested from 2006 to 2008, and the ZRay glider was tested from 2010 to 2014. As shown in Fig. 1, the ZRay glider was able to demonstrate a lift-to-drag (L/D) ratio of 20:1 during at sea testing.

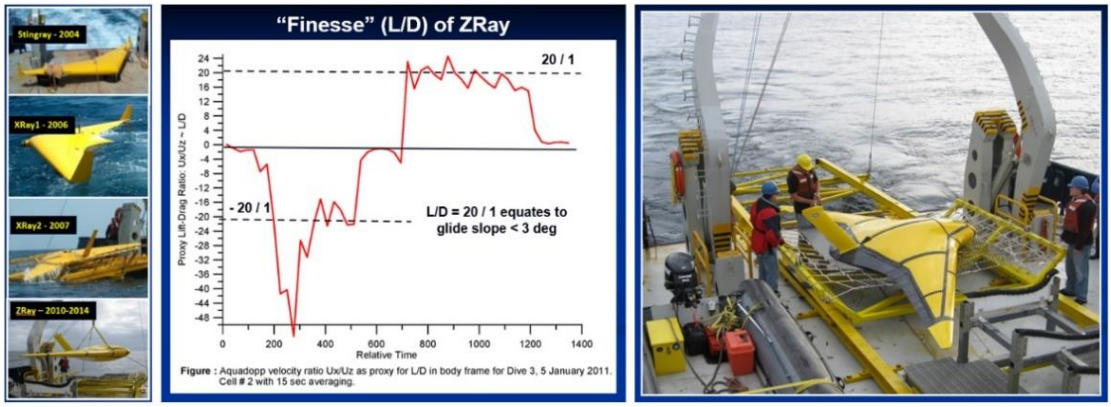

Fig. 1: The blended wing glider program led by SIO tested several gliders (left) and was able to verify the ZRay's L/D ratio of 20:1 (middle) during at-sea testing (right).

GA-EMS has been working with SIO to integrate an advanced power and energy system featuring a fuel cell and a GA-EMS pressure tolerant battery. This upgrade, as well as a modified hydrophone layout, was tested at sea in 2024 and 2025.

OPTIMIZATION OF UNDERSEA ACOUSTIC SURVEILLANCE PLATFORM

Silent operation and extended persistence of a UUV are two of the most important features of an undersea acoustic surveillance platform. Gliders are inherently quieter than prop-driven UUVs since the duty cycle of the pumps are 2-3% of the duty cycle of a propeller. Extended persistence is accomplished by optimizing the UUV's hydrodynamic efficiency and by implementing a power and energy system with a high energy density.

Maximizing the transit efficiency is accomplished hydrodynamically by minimizing the amount of lost kinetic energy. A hydrodynamically optimized winged glider leads to significantly less drag than a standard propeller-driven UUV [2]. Further hydrodynamic optimization of a glider is based on the mission goals. Gliders generally fall into one of two classes: 1) "profiling gliders" that have steep dive angles and are generally used to sample water column data; and 2) "cross country gliders" that are optimized to have the greatest horizontal transport efficiency. The "profiling gliders" such as the Spray [3], Seaglider [4], and Slocum [5] are based on a body of revolution with wings. A "cross country glider" with a blended wing utilizes the entire outer surface of the glider to generate lift. Since the lift-to-drag ratio is inversely proportional to the energy required to transit a certain horizontal distance, the vehicle's lift-to-drag ratio needs to be maximized to minimize the propulsion energy. GA-EMS developed a computational-fluid-dynamics-based software package to analyze glider performance as a function of 15 non-dimensionalized parameters. Utilizing a mix of proprietary and industry standard tools, a glider optimization tool was developed. This tool agrees qualitatively with previous analytical results in the literature [2], showing that blended wing gliders exhibit up to 40% better range than body-of-revolution gliders, whereas body-of-revolution gliders are better for faster speeds.

In addition to the optimization of the vehicle's form factor, persistence can be increased through maximizing the vehicle's energy storage. Power hungry sensors and systems, and the desire for longer range and more time on station, drive up the energy demand. The ultimate goal of realizing unlimited persistence through energy harvesting is under investigation [5,6]; however, it is yet to be widely utilized in underwater vehicles. The added complexity, size, and weight of the energy harvesting system needs to be accounted for, and the source of the energy harvesting will dictate where (geographically and in the water column) and how the vehicle can operate. The added complexity, strain on vehicle requirements, and operational limitations have generally led to battery powered vehicles.

GA-EMS specializes in developing safe, reliable power and energy systems for extreme environments. GA-EMS has developed a Lithium-ion Fault Tolerant (LiFT^{TM}) battery that prevents uncontrolled cascading failure, and a pressure tolerant battery (Fig. 2).

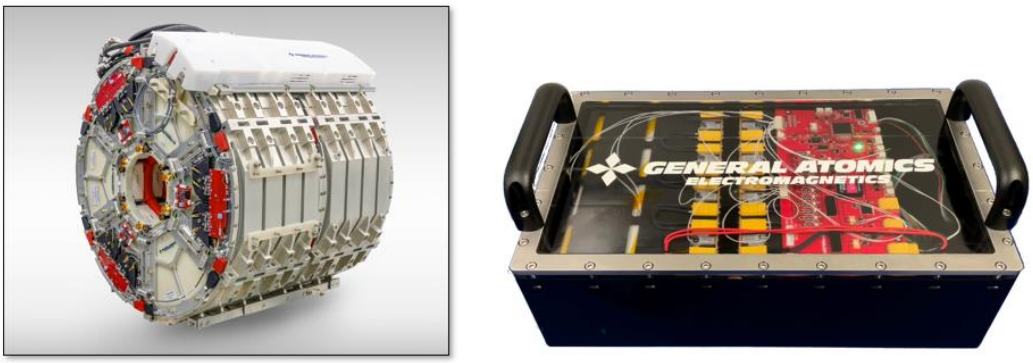

Fig. 2: The GA-EMS LiFT^{TM} battery (left), and pressure tolerant battery (right).

The LiFT^{TM} battery ensures the safety of personnel and equipment while keeping power available for high mission assurance. The assumption is that at some point, a lithium-ion cell is going to go into thermal runaway, and the LiFT^{TM} system will protect the remainder of the battery (and vehicle) from a catastrophic failure. The LiFT^{TM} system has been approved for use by the U.S. Navy for certain platforms.

GA-EMS has also developed a pressure tolerant battery capable of operation at full ocean depth. The absence of a pressure vessel enables an energy dense battery that can be conformal to a desired shape. This battery utilizes a dielectric fluid that aids with cell cooling, while also preventing fires and thermal runaway in the case of a cell failure. The fluid is also less dense that water, reducing the battery's overall weight in water.

Fuel cell systems have been under development for decades and have recently experienced exponential growth in the commercial sector driven by the transportation industry. A fuel cell system stores several times the energy of a battery of comparable size and weight. GA-EMS used a 300 W Baltic fuel cell and built the balance of plant to feed it reactants and manage the products. This custom fuel cell system, and the GA-EMS pressure tolerant battery were integrated into the ZRay and tested in February of 2025 (Fig. 3).

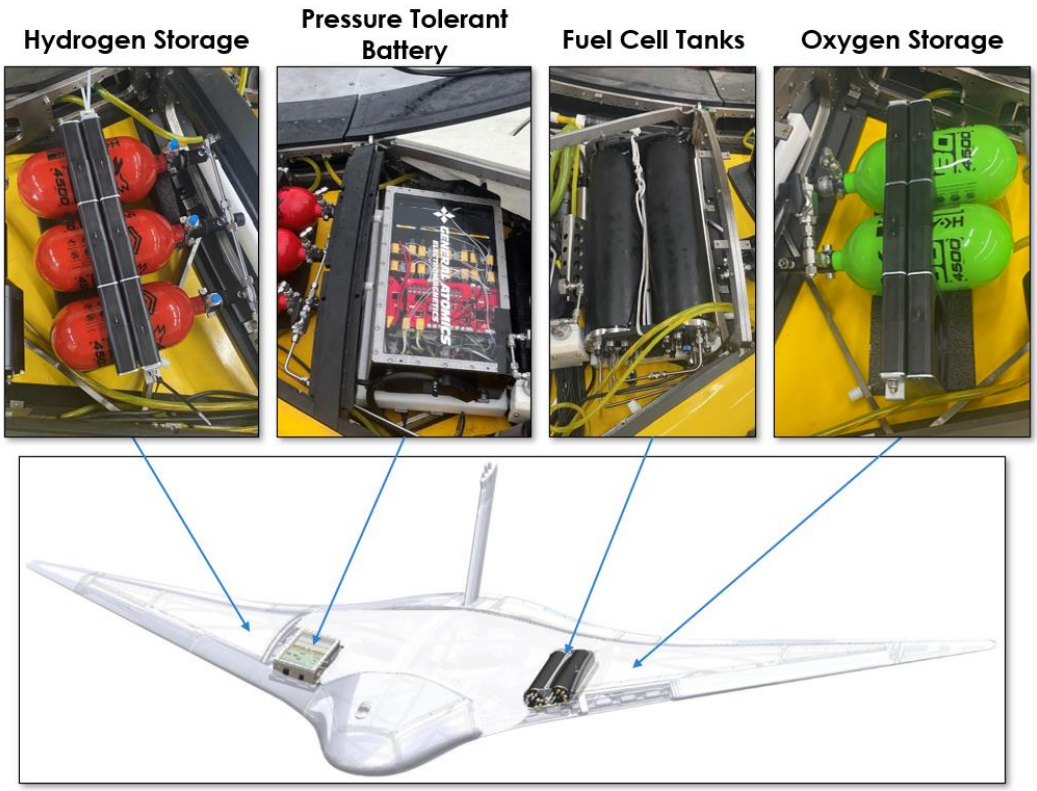

Fig. 3: ZRay hybridized with a GA-EMS pressure tolerant battery and fuel cell system.

Leveraging decades of work in fuel cell and battery development, this hybridized power and energy system significantly enhanced the energy density of the UUV. These advanced power and energy systems paired with the blended wing glider body enable an acoustic sensing platform with unprecidented persistence.

THE GLIDER AS AN ACOUSTICS PLATFORM

The ZRay glider was outfitted with passive hydrophone arrays inside the outer shell (see Fig. 4) for at-sea testing to demonstrate its acoustic surveillance capabilities.

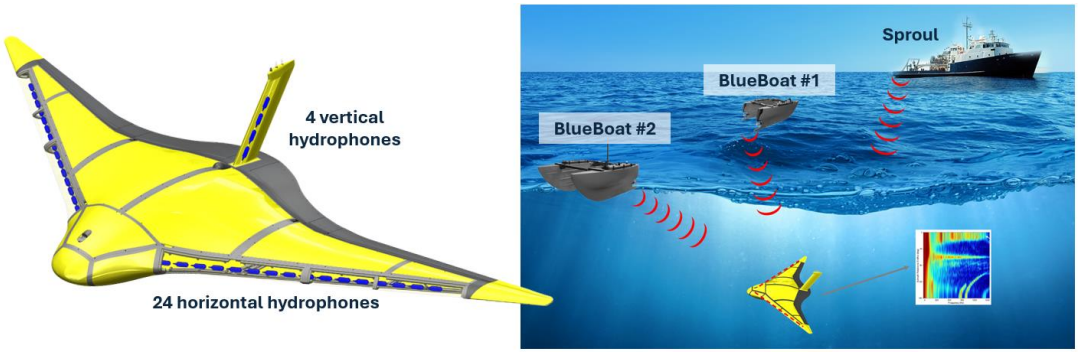

Fig. 4: The ZRay has been outfitted with multiple passive acoustic sensor systems.

The hydrophones are installed with 0.15 m inter-element spacing (half-wavelength spacing at 5 kHz). Each element is individually wrapped in open-cell foam to decrease the effects of non-acoustic pressure fluctuations (see below). The data acquisition system calibration curve in amplitude and phase has been calculated theoretically and parts of it have been confirmed by laboratory measurements. The effects of the analog to digital (A/D) converter settling time (i.e., the time delay in acquiring data samples across the array) are negligible up to 5 kHz, as determined by comparing results using time-aligned versus non-aligned time series input. Electronic self-noise of the system has been measured at sea and is more than 15 dB below ocean background noise above 7 Hz. A/D converter quantization noise is another 15 dB or more below electronic self-noise and so can be ignored.

The performance of passive acoustic arrays that move relative to the surrounding water can be adversely affected at low frequencies by noise from turbulent pressure fluctuations. This flow noise has much smaller spatial scales of coherence than low-frequency sound, so that coherence squared estimates between pairs of array elements can be used as a diagnostic of this contamination. As an example, Fig. 5 shows the spatial coherence squared levels for three time periods in the May, 2024 sea test, when the glider speed through the water was 0.14 m/sec (left), 0.4 m/sec (middle), and 0.5 m/sec (right). Note that coherence squared between any element and itself is unity across the band, explaining the horizontal solid red bar at reference element 9 in the three plots. In addition, element 1 was non-functional and element 28 was a non-acoustic electronically-equivalent dummy to measure electronic self-noise, resulting in the horizontal dark blue bars at the top and bottom of each plot.

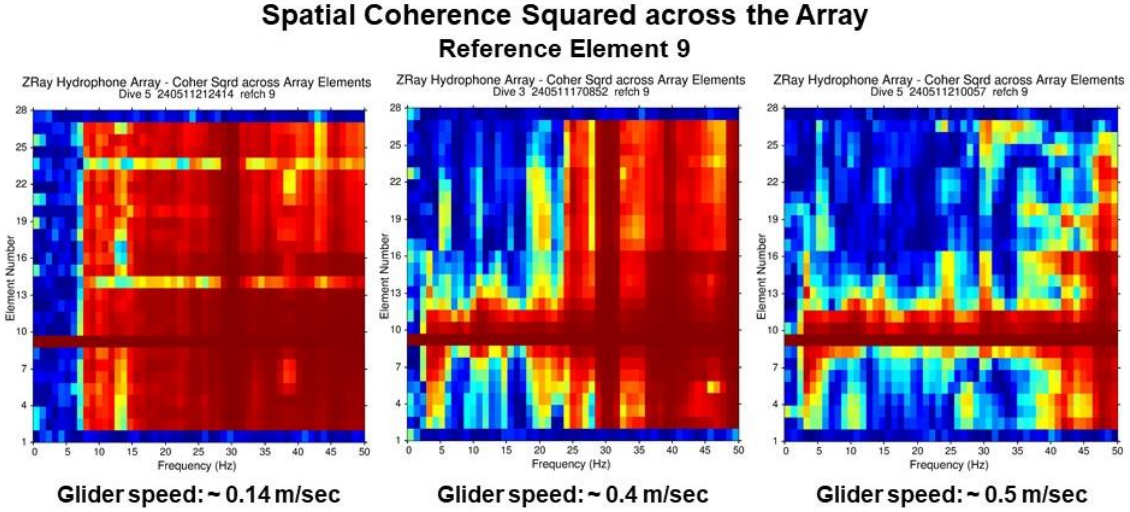

Fig. 5: Spatial coherence squared estimates between element 9 and all other hydrophones in the leading-edge array (elements 1-28 along the vertical axis) as a function of frequency (horizontal axis) from DC up to 50 Hz for three time periods in the May, 2024 sea test. The coherence squared values vary from 0 (dark blue) to 1 (dark red).

The level of coherence drops off rapidly with distance away from the reference (element 9) at the lowest frequencies (the blue areas above and below the dark horizontal red bar), and the frequency band of this rapid decay increases with increasing glider speed. The pressure spectral density curves over this low-coherence band are well fit by Eq. (8) of Strasberg, 1979, i.e.:

$$S_P(f) = 119 + 37 \bullet \log_{10}(U) - 27 \bullet \log_{10}(f) \quad (1)$$

which is derived assuming that pre-existing ocean turbulence of a given level (obtained from published ocean turbulence measurements) is advected past the hydrophones by fluid flow with relative speed *U*. In this equation, *U* has units of kts and the spectral density has the standard units of dB re 1 μPa²/Hz. Any turbulence generated by the glider itself is minimized by its wing shape and placement of the hydrophones in the leading edge.

Controlled acoustic sources (Lubell LL916) were deployed from autonomous surface vehicles ("BlueBoats") in all experiments to allow evaluation of array localization performance. These sources were suspended about 1 m below the sea surface and repeatedly transmitted a 60-sec waveform comprised of a) a set of 7 tones for 40 sec, followed by a 1-sec gap, and then b) an 18-sec-duration linear frequency modulated (LFM) upsweep, ending in a 1-sec gap. The latitude/longitude positions of these acoustic sources along with those of the ZRay glider and the R/V Sproul are plotted in Fig. 6 for two 1-min time periods in the Aug, 2024 (left plot) and Feb, 2025 (right plot) sea tests.

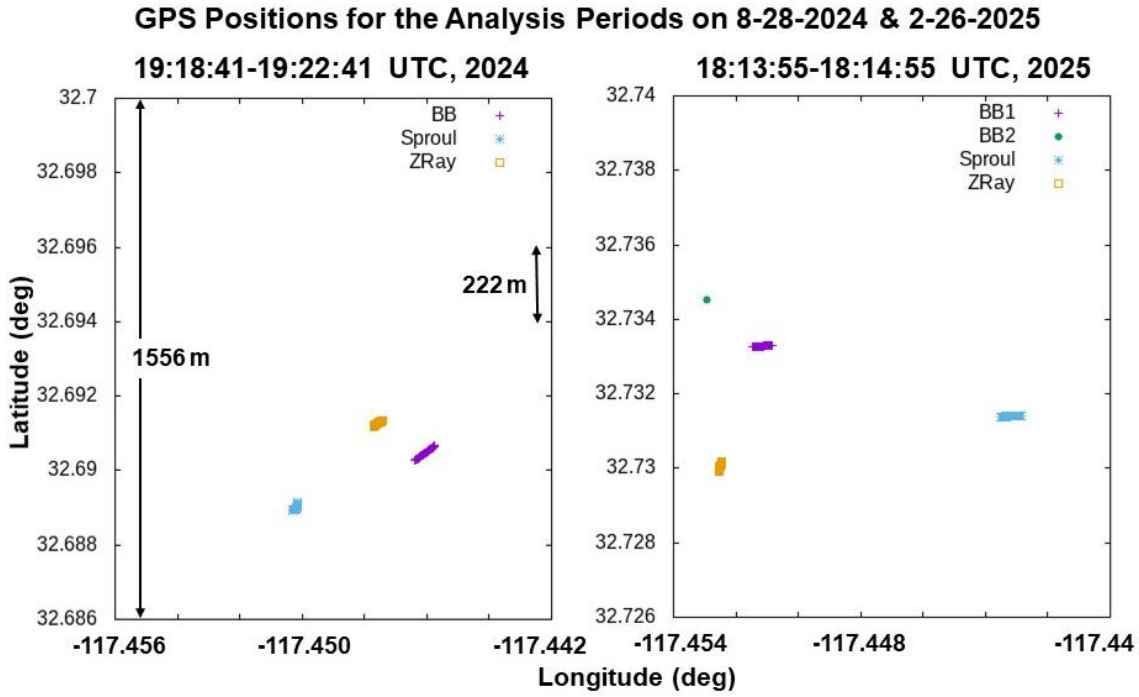

Fig. 6: The dead-reckoned positions in latitude and longitude of ZRay (gold), the BlueBoat vehicles with controlled acoustic sources (labelled "BB": purple, "BB1": purple, and "BB2": green), and the R/V Sproul GPS fixes (light blue).

Two BlueBoat ("BB") sources were deployed simultaneously during the 1-min time period in the February, 2025 sea test shown in the right plot in Fig. 6. These sources transmitted the same 40-sec comb of 7 tones, but starting at different times in the 60-sec cycle. In addition, their 18-sec LFM waveforms differed so that matched filtering of the

received time series allowed the 18-sec part of the 60-sec period that each source transmitted its LFM upsweep to be identified. Results of beamforming in azimuth at two tone frequencies over this 1-min period is shown in Fig. 7.

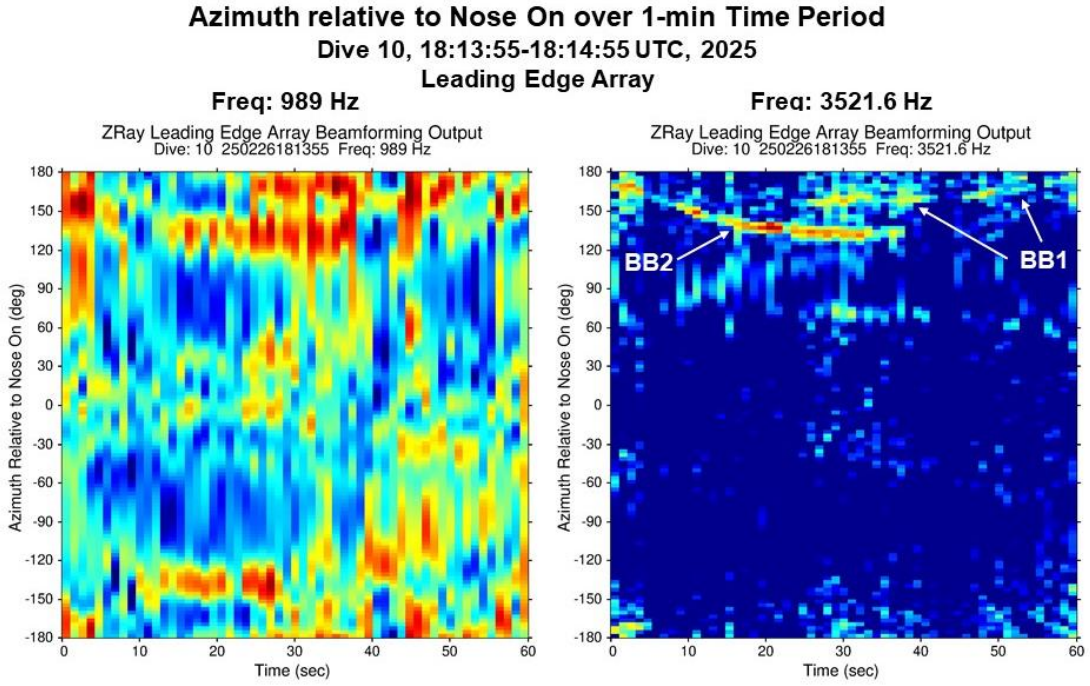

Fig. 7: White-noise-constrained adaptive beamforming output as a function of azimuth relative to glider heading (vertical axis) and time into a 1-min period (horizontal axis) at two tone frequencies – 989 Hz (left plot) and 3522 Hz (right plot). Positive azimuth angles represent angles to the starboard side and negative azimuths represent angles to port.

Two tracks on the starboard side of the glider (i.e., at the positive azimuth angles in the upper half of each plot) can be identified in the plots in Fig. 7. The azimuths of these tracks are consistent with the bearings of the BlueBoat acoustic sources from ZRay in Fig. 6 combined with the heading of ZRay to the south-southwest during this period. In fact, the sagging nature of the tracks in Fig. 7 is caused by the rotation of the glider heading from 180º true to 210º true and then back over this 1-min period. The matched-filter output indicates that BB1 transmitted its LFM upsweep over the initial third or so of the 60-sec period, so that it transmitted the 7-tone comb over the final two-thirds. In contrast, BB2 transmitted its LFM waveform over the final third and the 7-tone comb during the initial two-thirds. Therefore (as the labeling in white font in the right-hand plot of Fig. 7 indicates), the track at smaller azimuths over the initial portion of the 1-min period is that of the BB2 source, whereas the track near aft end-fire on the starboard side over the final two-thirds is the BB1 source. This separation in azimuth angle of the two sources again is consistent with the positions of the sources relative to the glider in the right-hand plot in Fig. 6.

In addition to the leading-edge hydrophone array, four hydrophone elements were placed inside the ZRay antenna mast to create vertical aperture, as illustrated in Fig. 4. An example of the beamforming output in elevation angle from this 4-element array is presented below. The data were collected over a 1-min period in the Aug, 2024 sea test. The left plot in Fig. 6 provides the locations of ZRay, the BlueBoat source, and the R/V Sproul over this 1-min period, showing the glider was less than 200 m from the source. The elevation angle of the arrival at 2623 Hz over this 1-min period is presented in Fig. 8.

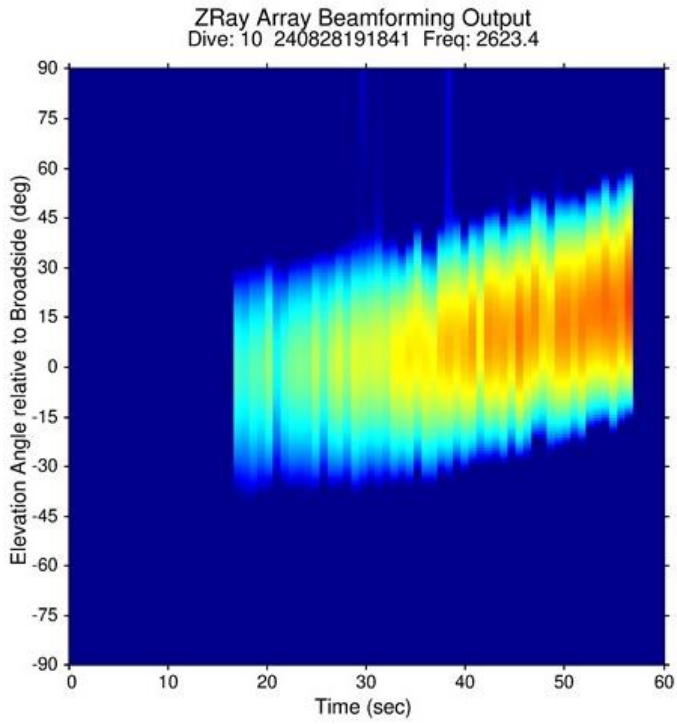

Fig. 8: White-noise-constrained adaptive beamforming output at a tone frequency of 2623 Hz as a function of elevation angle relative to the horizontal (vertical axis) and time into a 1-min period (horizontal axis). Positive elevation angles are upward looking and negative angles are downward looking.

The evolution of the arriving energy to higher elevation angles over time is partly due to the progressively increasing depth of the glider during this time, and partly due to a steadily increasing bias as a result of beamforming mismatch - the beamformer look direction in azimuth was fixed over the 1-min period, whereas the glider rotated in heading by nearly 30˚.

A detection/classification/localization/tracking (DCLT) algorithm string presently is being automated for real-time on-board array processing in future sea tests. It will allow rapid quantitative analyses of processing performance. In GA-EMS's next generation blended wing glider (GRay) outputs from this DCLT algorithm string will be communicated directly to the flight control computer to allow real-time adaptation of mission parameters based on the glider's measurements of the ocean sound field.

NEXT GENERATION GLIDER UNDER CONSTRUCTION

GA-EMS is presently designing and fabricating the next generation blended wing glider, GRay. This vehicle is comparable in wingspan to ZRay; however, advances in electronics, sensors, and batteries have enabled a significant payload bay in the GRay, as shown in Fig. 9. The body is slightly enlarged, while being mindful to minimize hydrodynamic degradations. The available cargo space is roughly 8 ft^3, cargo can be released through the top or bottom of the vehicle, and has 5, 12, 24, and 48 VDC available. This vehicle will be fabricated by the end of 2025, and at-sea testing will begin in 2026.

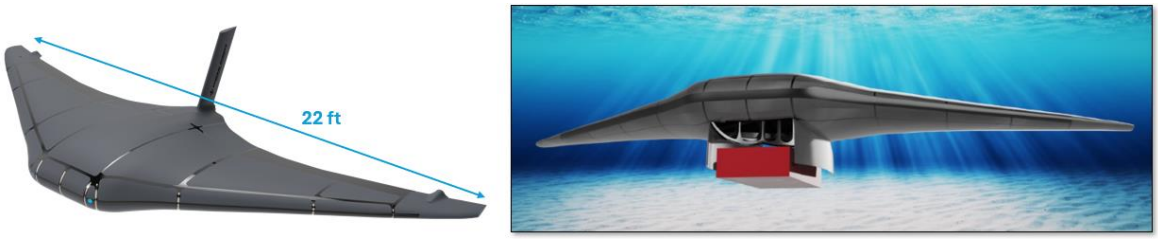

Fig. 9: The GA-EMS GRay glider being fabricated in 2025.

CONCLUSIONS

Persistence in underwater surveillance can be achieved through careful engineering design and implementation of appropriate subsystems. By optimizing the design of a blended wing glider, and integrating energy-dense energy storage systems, the blended wing glider can have extraordinary range and time on station. Due to how a buoyancy-driven glider operates, the vehicle is acoustically (and electromagnetically) virtually silent for the vast majority of the operational time, making it an ideal acoustic sensor platform. GA-EMS is working with SIO to hybridize the ZRay glider with a battery and fuel cell system, significantly increasing the persistence. GA-EMS is also fabricating a next generation GRay glider that will have a sizable payload bay for sensors and payloads. GA-EMS and SIO will be testing these vehicles at sea several times a year for the next few years, aiming to develop novel acoustic sensing capabilities. GA-EMS is looking for novel sensors that can be deployed and tested on the GRay to demonstrate future capabilities of a much larger glider.

ACKNOWLEDGEMENTS

The authors would like to thank GA-EMS for funding the recent glider work, as well as the technical team at SIO, particularly Dennis Rimington and Dave Price for their tireless work on the refurbishment and operation of the ZRay.

REFERENCES

[1] **G. L. D'Spain**, Final Report, https://apps.dtic.mil/sti/pdfs/ADA496168.pdf, *Office of Naval Research, 2009.*

[2] **Jenkins, S. A. and G. L. D'Spain**, *Springer Handbook of Ocean Engineering*, M. Dhanak and N. Xiros, Springer Cham, 301-321, 2016.

[3] **J. Sherman, R. Davis, W. Owens, J. Valdes**, The autonomous underwater glider Spray, *IEEE J. Oceanic Engin.,* 26 (4), 437-446, 2001.

[4] **C. Eriksen, T. Osse, R. Light, T. Wen, T. Lehman, P. Sabin, J. Ballard, A. Chiodi**, A long-range autonomous underwater vehicle for oceanographic research, *IEEE J. Oceanic Engin.,* 26 (4), 424-436, 2001.

[5] **D. Webb, P. Simonetti, C. Jones**, SLOCUM: An underwater glider propelled by environmental energy, *IEEE J. Oceanic Engin.*, 26 (4), 447-452, 2001.

[6] Y. Chao, Autonomous underwater vehicles and sensors powered by ocean thermal energy. In OCEANS 2016-Shanghai, pp. 1-4. IEEE, 2016.

[7] M. Strasberg, Nonacoustic noise interference in measurements of infrasonic ambient noise, *J. Acoust. Soc. Am.,* 66 (5), 1487-1493, 1979.